Electronic Supplementary Information

New Journal of Chemistry

Stability and Decomposition of Copper(I) Boryl Complexes: [(IDipp)Cu–Bneop], [(IDipp*)Cu–Bneop] and Copper Clusters

Wiebke Drescher, Corinna Borner and Christian Kleeberg*

Institut für Anorganische und Analytische Chemie,
Technische Universität Braunschweig,
Hagenring 30, 38106 Braunschweig, Germany.

* Author E-mail Address: ch.kleeberg@tu-braunschweig.de

Contents

1. a. Decomposition of [(IDipp)Cu–Bneop] (**2**)
   • NMR Data S2
   • X-ray Powder Diffraction Data S4
   b. Decomposition of [(IDipp*)Cu–Bneop] (**3**) – NMR Data S5

2. Crystal Structure Determination Data S6
   a. Hirshfeld Surface Plots of **2** from **2**(PhMe) and of **3** S8
   b. Structural Data of **2**(THF) S9
   c. Structural Data of $[(IDipp)_2Cu][Bneop_2]$ S10
   d. Additional Structural Data of $[(IDipp)_6Cu_{55}]$ S11
   e. Additional Structural Data of $[(IDipp)_{12}Cu_{179}]$ S12

3. Additional Full NMR Spectra
   a. [(IDipp)Cu–Bneop] (**2**) S16
   b. [(IDipp*)Cu–Bneop] (**3**) S22

References S24

1a. Decomposition of [(IDipp)Cu–Bneop] (**2**)

NMR Data

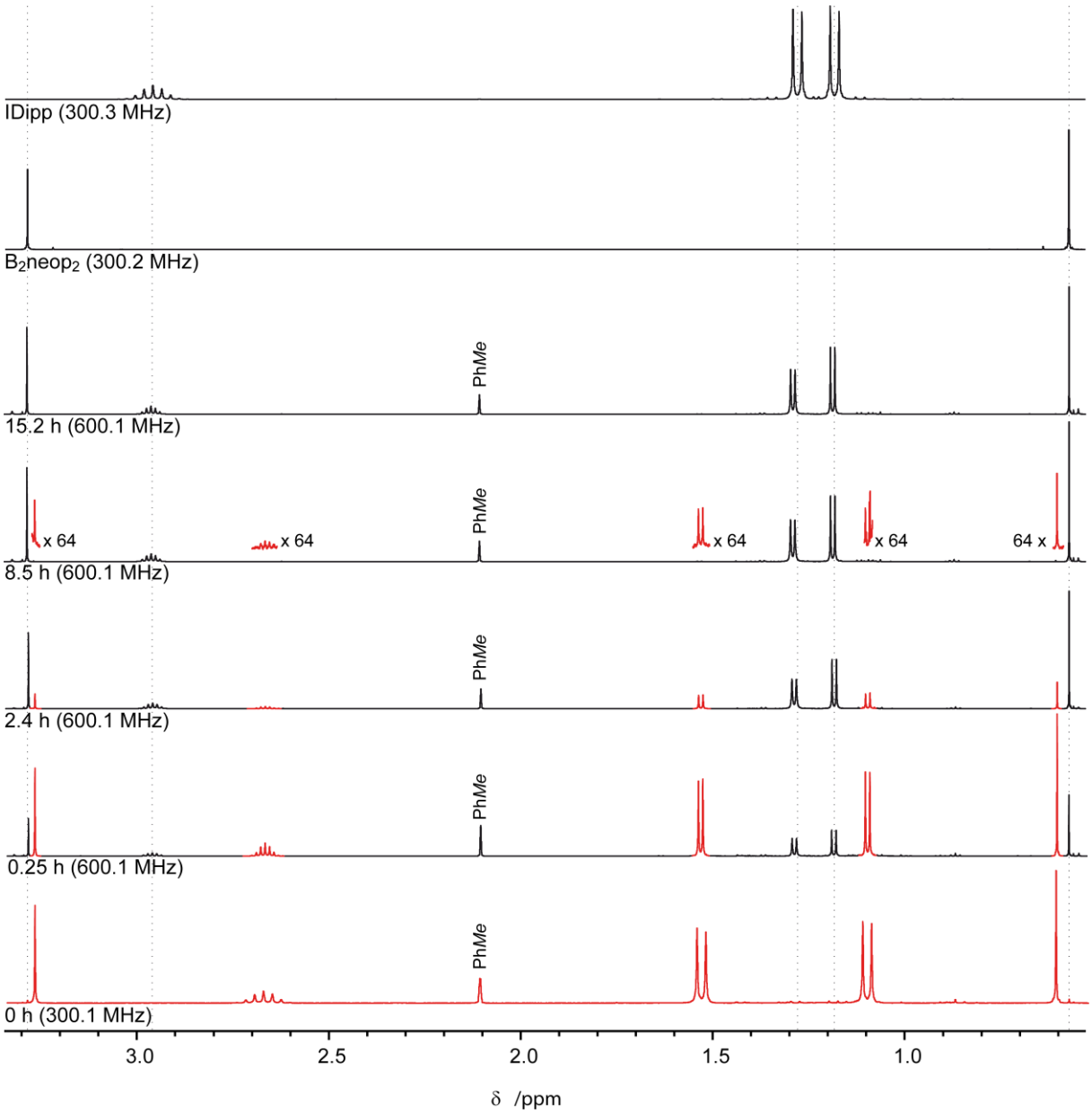

Figure S1a: Decomposition of **2** at room temperature monitored by ^{1}H NMR spectroscopy (C_6D_6, rt).

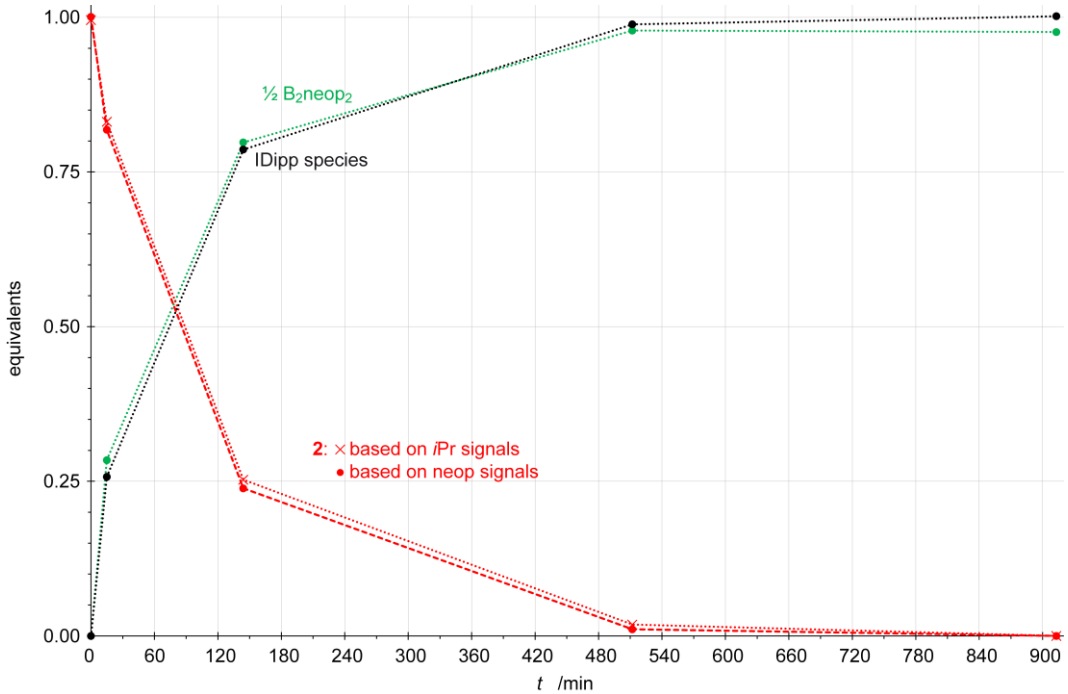

Figure S1b: Kinetics of the decomposition of **2** based on the ^{1}H NMR spectroscopic data.

X-ray Powder Diffraction Data

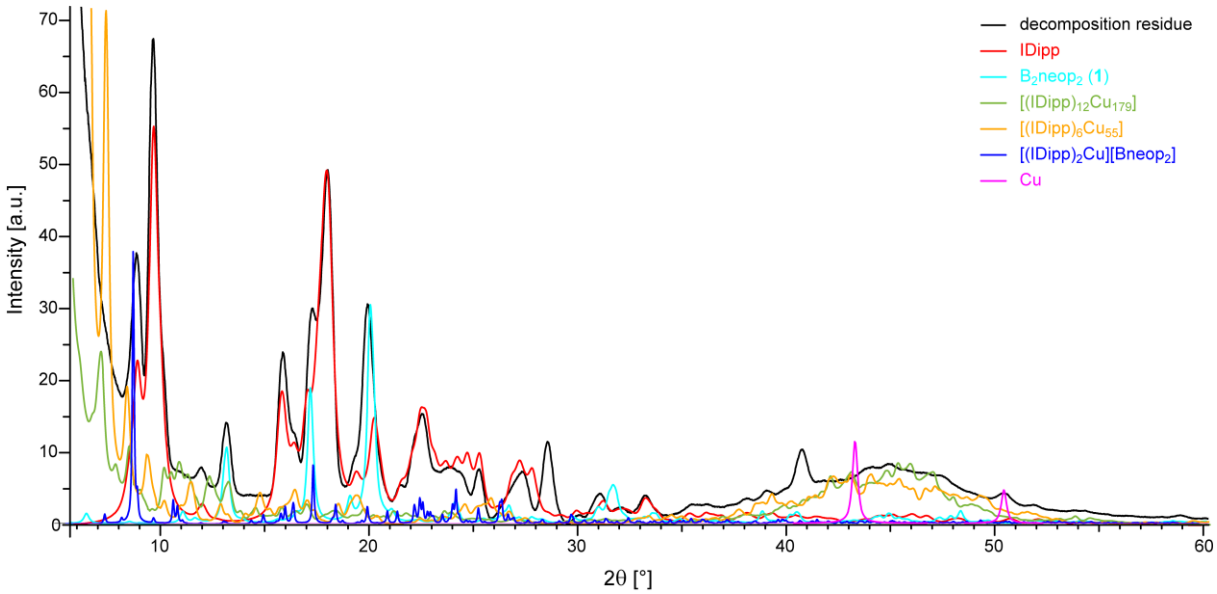

Figure S2: Powder diffraction pattern of the decomposition residue of **2** and calculated patterns of potential decomposition products.[S1]

A qualitative comparison of the diffraction pattern obtained from the decomposed residue with potential decomposition products (Figure S2) shows, that the free carbene IDipp and the diborane(4) **1** are, in agreement with the NMR data, unambiguously present. The presence of the low-valent copper clusters $[(IDipp)_6Cu_{55}]$ and $[(IDipp)_{12}Cu_{179}]$ as well as of elemental copper is not clearly corroborated. However, a broad feature in the range $35° \leq 2\theta \leq 55°$ as also found in the calculated diffraction patterns for $[(IDipp)_6Cu_{55}]$ and $[(IDipp)_{12}Cu_{179}]$ may suggest the presence of these or related copper clusters. Moreover, the recorded diffraction pattern exhibits additional signals that are at present not accounted for, indicating the presence of additional not identified species.

Experimental Part: [(IDipp)Cu–O*t*Bu] (150 mg, 289 μmol, 1.0 eq) and **1** (65 mg, 287 μmol, 1.0 eq) were combined in PhMe (8 mL) and kept at room temperature for >24 h, all volatiles were removed *in vacuo* and the blackish residues thoroughly dried *in vacuo*. A sample of the powdered residues was transferred under an atmosphere of nitrogen into a glass capillary (∅ 0.5 mm), which was flame-sealed, and a powder diffraction pattern was recorded using a *Rigaku Oxford Diffraction Synergy-S* instrument with mirror-focused CuK_α radiation (beam diameter approx. 0.15 mm) using the CrysAlisPro software package. The sample was rotated during the measurement. Under identical conditions, the diffraction pattern of an empty capillary was recorded and subtracted to account for the diffuse background scattering of the glass.

1b. Decomposition of [(IDipp*)Cu–Bneop] (**3**) – NMR Data

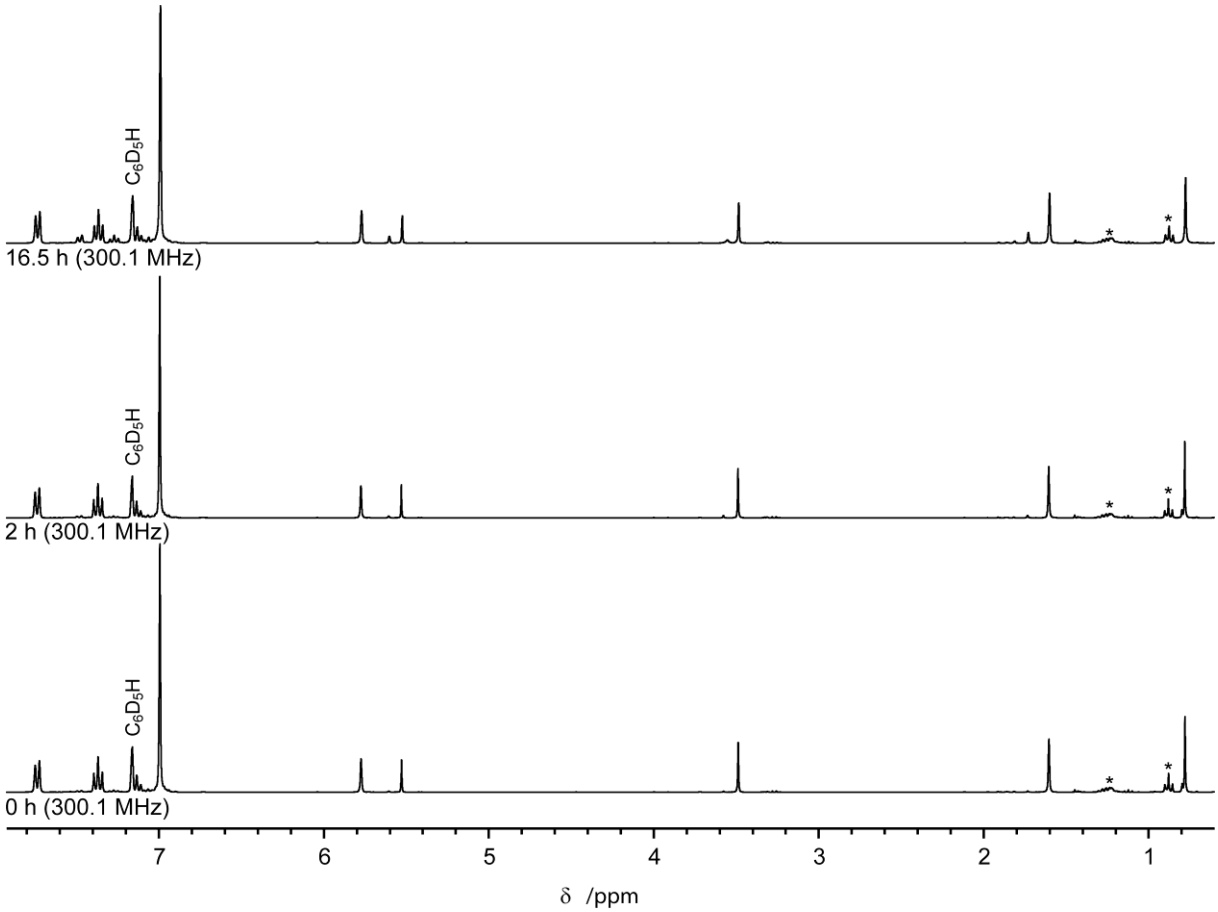

Figure S3: Stability of **3** at room temperature monitored by ^{1}H NMR spectroscopy (C_6D_6, rt, **n*-pentane).

2. Crystal Structure Determination Data

Table S1. Crystallographic data collection parameters for **2**(PhMe), **2**(THF) and **3**.

	2(PhMe)[a]	**2**(THF)[b]	**3**
Source	reaction mixture	recryst. **2**(PhMe)	reaction mixture
Cryst. cond.	C_7H_8/C_5H_{12}, –40 °C	THF/C_5H_{12}, –40 °C	Et_2O, rt (evaporation)
Composition	$C_{32}H_{46}BCuN_2O_2$ (C_7H_8)	$C_{32}H_{46}BCuN_2O_2$ (C_5H_8O)	$C_{74}H_{66}BCuN_2O_2$
Mass (g mol^{-1})	657.19	637.16	1089.63
Cryst. size (mm^3)	0.18 × 0.09 × 0.03	0.23 × 0.10 × 0.07	0.161 × 0.122 × 0.051
description	colourless plate (frag.)	colourless needle	clear colourless frag. of lathe
Crystal system	triclinic	monoclinic	orthorhombic
Space gr. (no.)	$P\bar{1}$ (2)	$P2_1/n$ (14)	*Pbca* (61)
Z, Z'	4, 2	4, 1	8, 1
a (Å)	12.4025(14)	10.6114(2)	10.8381(1)
b (Å)	14.8764(19)	15.0816(4)	25.8186(2)
c (Å)	20.461(2)	22.6645(5)	41.5657(3)
α (°)	93.490(9)	90	90
β (°)	96. 21(11)	93.438(2)	90
γ (°)	93.591(9)	90	90
Volume (Å^3)	3733.7(7)	3620.63(14)	11631.11(16)
D_{calcd} (Mg m^{-3})	1.169	1.169	1.245
T (K)	100(2)	100(2)	100(2)
Radiation, λ (Å)	CuK_α, 1.54184	CuK_α, 1.54184	CuK_α, 1.54184
μ (mm^{-1})	1.072	1.109	0.905
Reflections: all	24616	48009	187069
indep.	24616	7327	12343
obs. [$I > 2\sigma(I)$]	14196	6564	11299
2θ range (°)	3.57 – 67.00	3.52 – 77.96	3.42 – 77.83
Param. / Restr.	843 / 3	353 / 0	725 / 0
GooF on F^2	0.912	1.051	1.030
R_{int}	n/a	0.0415	0.0377
R_1 [$I > 2\sigma(I)$]	0.0605	0.0543	0.0423
wR_2 (all data)	0.1582	0.1598	0.0458
peak / hole (Å^{-3})	0.667 / –0.713	0.815 / –0.316	0.536 / –0.885
CCDC no.	2008213	2008217	2008216

[a] The crystal was non-merohedrally twinned by 180° rotation about the *b** axis and was refined as 2-component twin; the twin factor refined to 0.4380(8). [b] No appropriate model could be refined for the co-crystallised THF molecule; its contribution was removed mathematically from the dataset using the SQUEEZE algorithm as implemented in PLATON.[S2]

Table S1 (cont.). Crystallographic data collection parameters for $[(IDipp)_2Cu][Bneop_2]$, $[(IDipp)_6Cu_{55}]$ and $[(IDipp)_{12}Cu_{179}]$.

	$[(IDipp)_2Cu][Bneop_2]$	$[(IDipp)_6Cu_{55}]$[c]	$[(IDipp)_{12}Cu_{179}]$[d]
Source	reaction mixture	reaction mixture	decomposition of **2**(PhMe)
Cryst. cond.	THF, rt to –40 °C	PhMe, rt	Et_2O/C_5H_{12}, rt
Composition	$C_{64}H_{92}BCuN_4O_4$	$C_{162}H_{216}Cu_{55}N_{12}$	$C_{324}H_{432}Cu_{179}N_{24}$
Mass (g mol^{-1})	1055.76	5826.16	16037.94
Cryst. size (mm^3)	0.123×0.060×0.047	0.08 × 0.04 × 0.03	0.078×0.072×0.054
description	colourless rhombohedron	dark black prism	metallic black block
Crystal system	monoclinic	triclinic	monoclinic
Space gr. (no.)	*C*2/*c* (15)	$P\bar{1}$ (2)	$P2_1/n$ (14)
Z, Z'	4, ½	1, ½	2, ½
a (Å)	16.1031(3)	18.5018(11)	24.7078(3)
b (Å)	18.2156(3)	18.5259(12)	34.1167(6)
c (Å)	20.4319(4)	19.1587(12)	26.0758(3)
α (°)	90	72.233(6)	90
β (°)	97.627(2)	61.343(6)	93.7630(10)
γ (°)	90	82.045(6)	90
Volume (Å^3)	5940.2(2)	5487.4(7)	21933.2(5)
D_{calcd} (Mg m^{-3})	1.181	1.763	2.428
T (K)	100(2)	100(2)	100(2)
Radiation, λ (Å)	CuK_α, 1.54184	CuK_α, 1.54184	CuK_α, 1.54184
μ (mm^{-1})	0.891	5.788	9.235
Reflections: all	33152	62742	405489
indep.	6219	19165	45979
obs. [$I > 2\sigma(I)$]	5748	13158	31835
2θ range (°)	3.68 – 77.73	2.51 – 67.00	2.39 – 77.84
Param. / Restr.	345 / 0	1033 / 0	2733 / 0
GooF on F^2	1.048	1.061	1.046
R_{int}	0.0337	0.0532	0.0794
R_1 [$I > 2\sigma(I)$]	0.0390	0.0619	0.0520
wR_2 (all data)	0.0984	0.2022	0.1590
peak / hole (Å^{-3})	0.416 / –0.339	1.709 / –1.287	0.773 / –0.799
CCDC no.	2008214	2008215	2008218

[c] No appropriate model could be refined for co-crystallised solvent molecules; its contribution was removed mathematically from the dataset using the SQUEEZE algorithm as implemented in OLEX. A solvent mask was calculated and 336 electrons were found in a volume of 1580 Å^3 in 1 void per unit cell. This is consistent with the presence of 7 molecules of PhMe per Unit Cell which account for 350 electrons per unit cell.[S3,S4] [d] No appropriate model could be refined for the co-crystallised solvent molecules; its contribution was removed mathematically from the dataset using the SQUEEZE algorithm as implemented in PLATON. During this, 940 electrons were found in a volume of 3260 Å^3 per unit cell, consistent with the presence of 22 molecules of Et_2O and/or *n*-pentane per unit cell.[S2] [e] It was noted that the lath-shaped crystals of **3** tend to be twinned, as indicated by inspection under a polarisation microscope. The crystal structure determination was conducted on a 'mechanically detwinned' fragment.

2a. Hirshfeld Surface Plots of **2** from **2**(PhMe) and of **3**

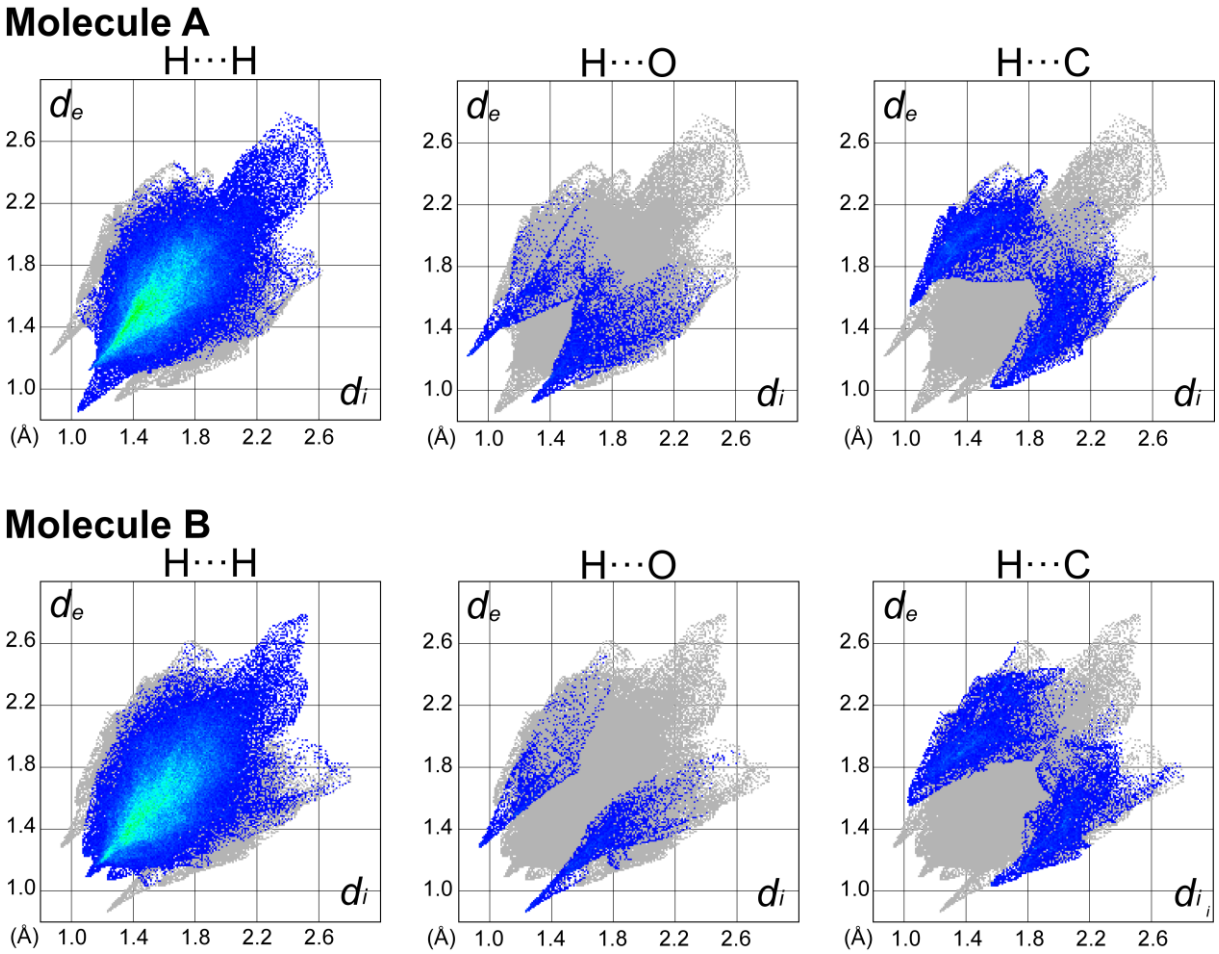

Figure S4: 2D Fingerprints plots of **2** from **2**(PhMe).

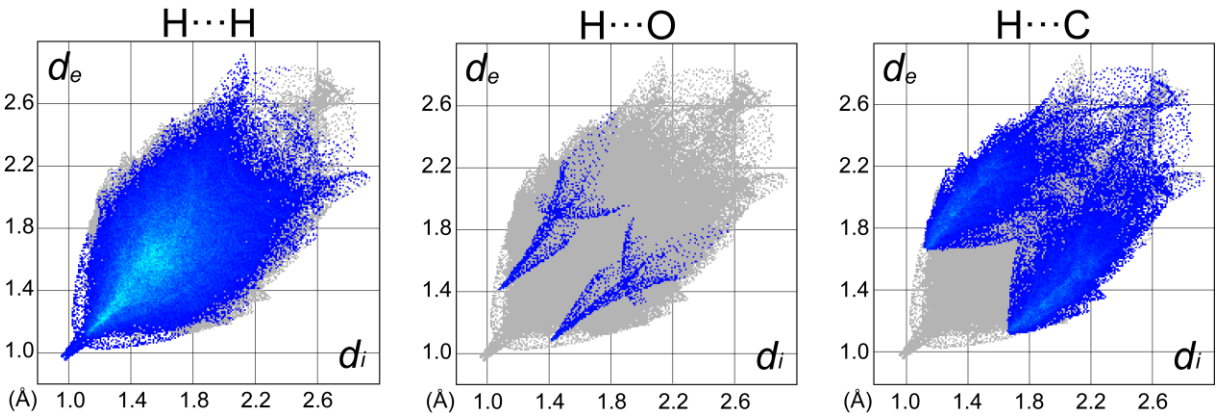

Figure S5: 2D Fingerprints plots of **3**.

2b. Structural Data of **2**(THF)

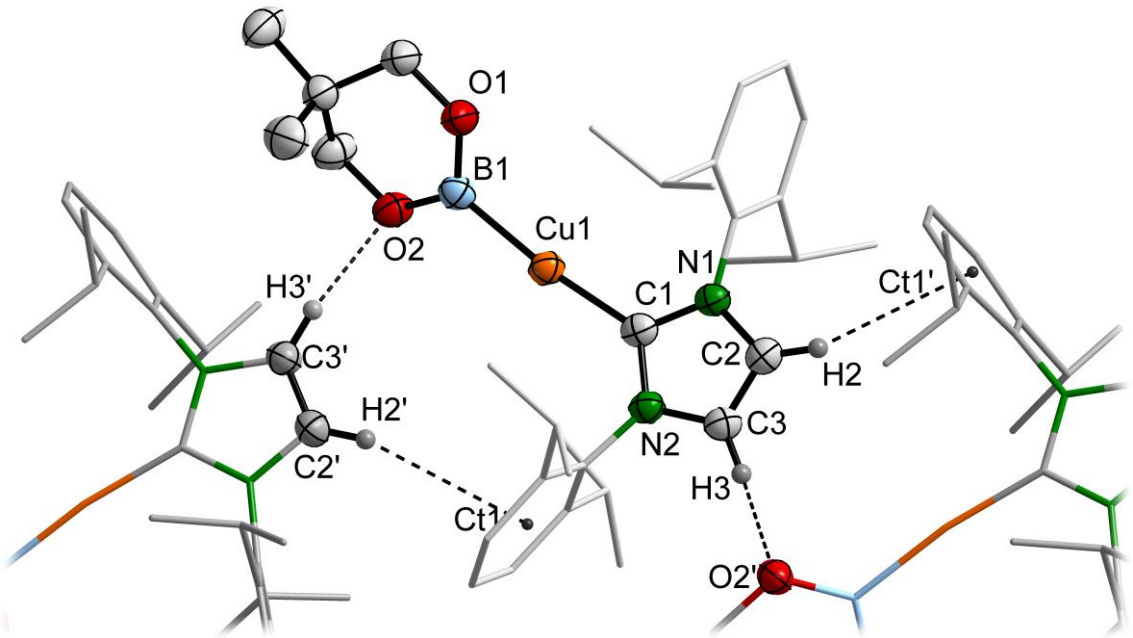

Figure S6: Section of the solid state structure of [(IDipp)Cu–Bneop] (**2**) from **2**(THF); ellipsoids at the 50% probability level, selected H atoms shown with arbitrary radius. Selected distances (Å) and angles (°): C1–Cu1 1.939(2), B1–Cu1 2.001(2), H3···O2' 2.339(1), C3···O2' 3.254(2), H2···Ct1' 3.1015(1), B1–Cu1–C1 172.45(9), C3···H3···O2' 161.3(1), ∠(N,C,N,Cu)/(O,B,O,Cu) 37.8(6).

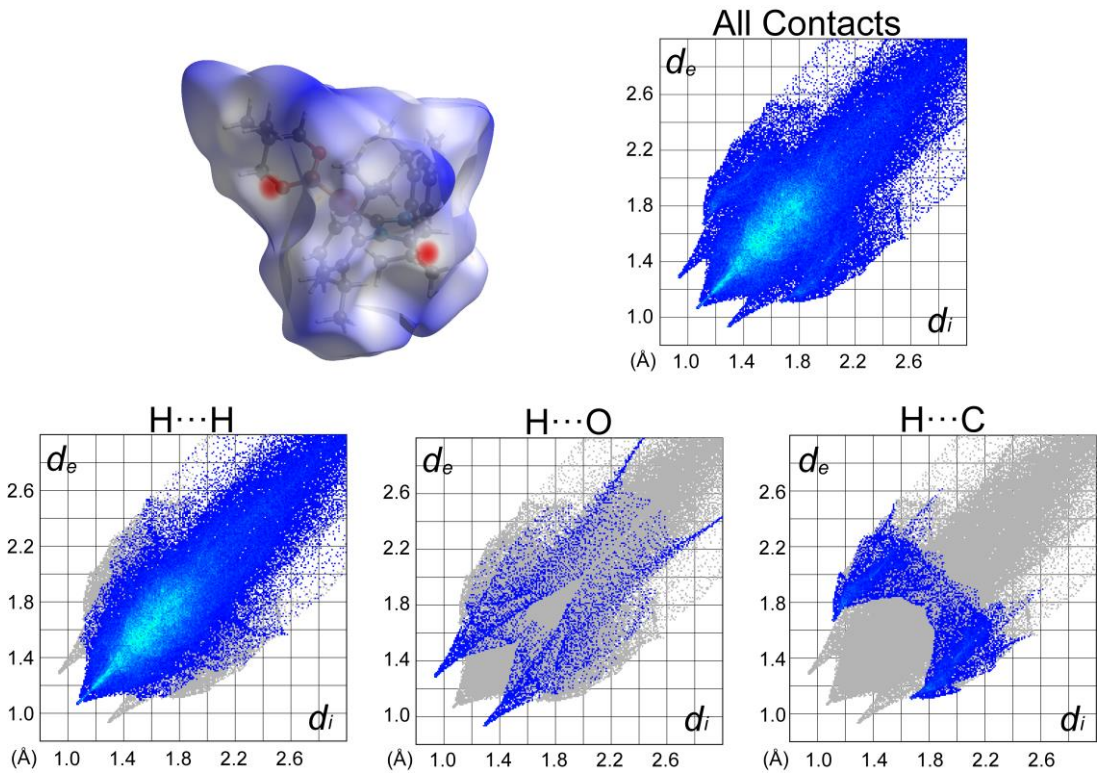

Figure S7: Hirshfeld surface and 2D Fingerprints plots of **2** from **2**(THF).

2c. Structural Data of $[(IDipp)_2Cu][Bneop_2]$

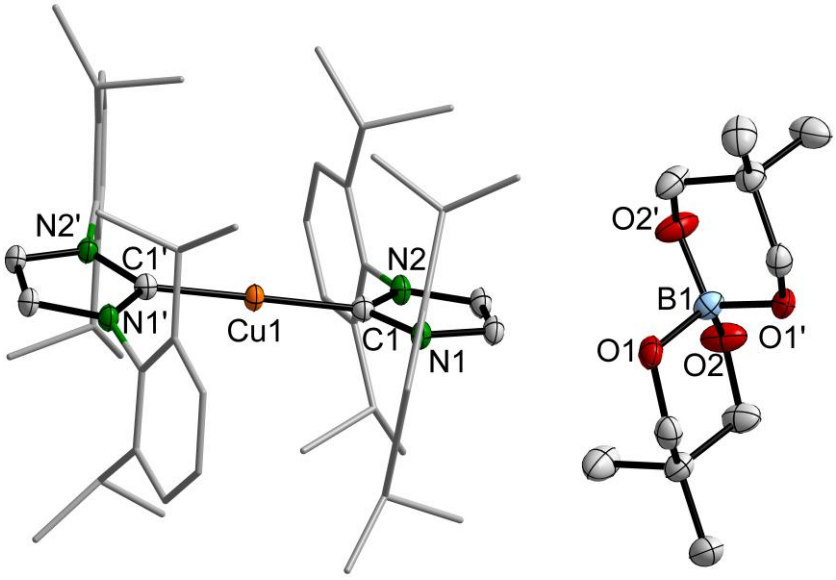

Figure S8: Solid state structure of $[(IDipp)_2Cu][Bneop_2]$; ellipsoids at the 50% probability level, H atoms omitted for clarity, prime indicates atoms generated by a 2-fold axis. Selected distances (Å) and angles (°): C1–Cu1 1.9204(14), C1–Cu1–C1' 179.43(8), ∠(N1,C1,N2,Cu1)/(N1',C1',N2',Cu1) 11.2(1), B1–O1 1.480(2), B1–O2 1.456(2), O1–B1–O2 111.70(7), O1–B1–O2 108.38(7), O1–B1–O1' 109.6(2).

2d. Additional Structural Data of $[(IDipp)_6Cu_{55}]$

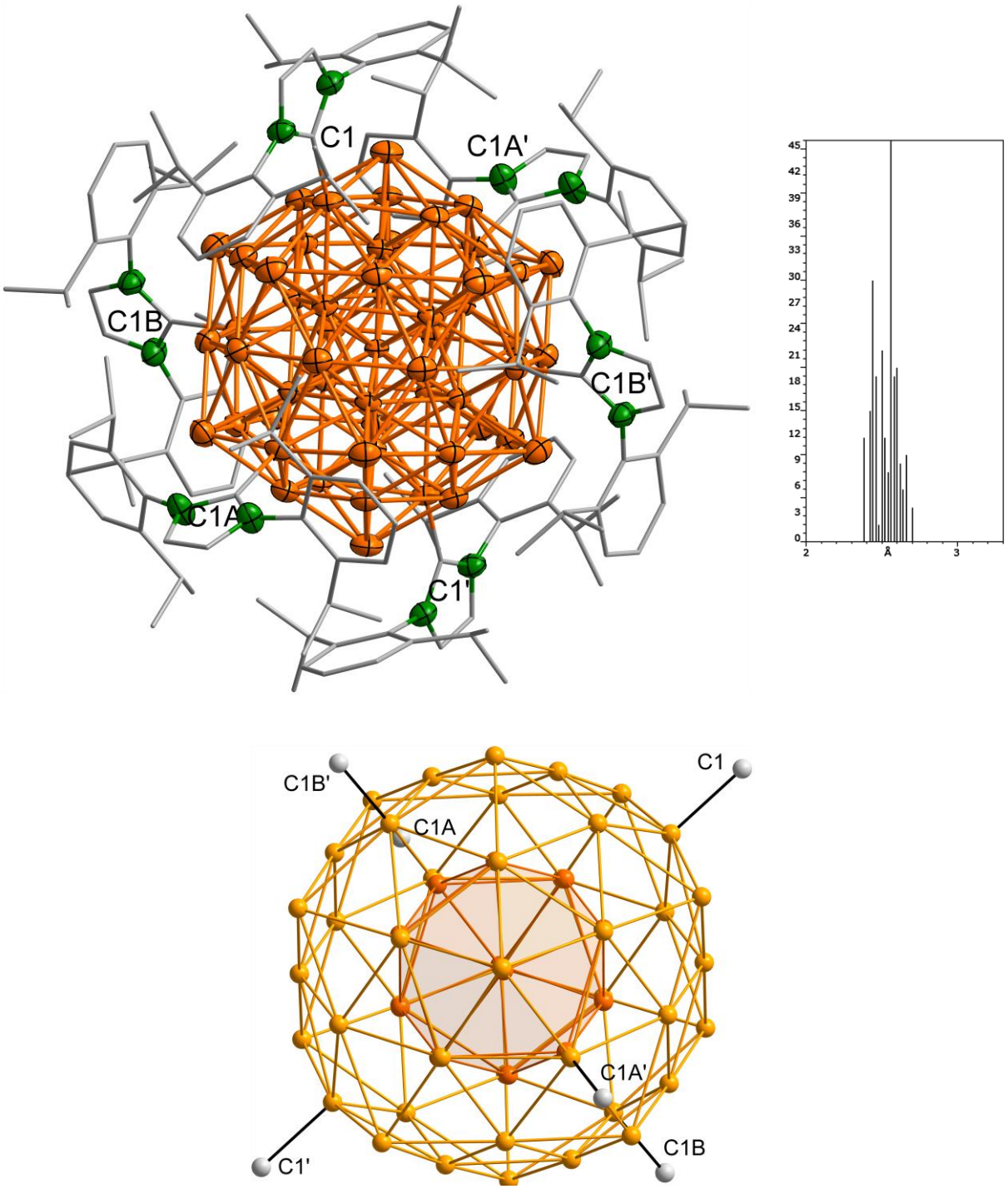

Figure S9: Views of the solid state structure of $[(IDipp)_6Cu_{55}]$. *Top:* Ellipsoids of the heteroatoms at the 50% probability level, carbon atoms with arbitrary radii, H atoms omitted for clarity (*inset:* histogram of the Cu···Cu distances in the Cu_{55} core). *Bottom:* View along the approximate five-fold axis, NHC only represented by their carbene carbon atoms (grey); all atoms with arbitrary radii, H atoms omitted for clarity. Primes indicate atoms generated by inversions.

2e. Additional Structural Data of [(IDipp)$_{12}$Cu$_{179}$]

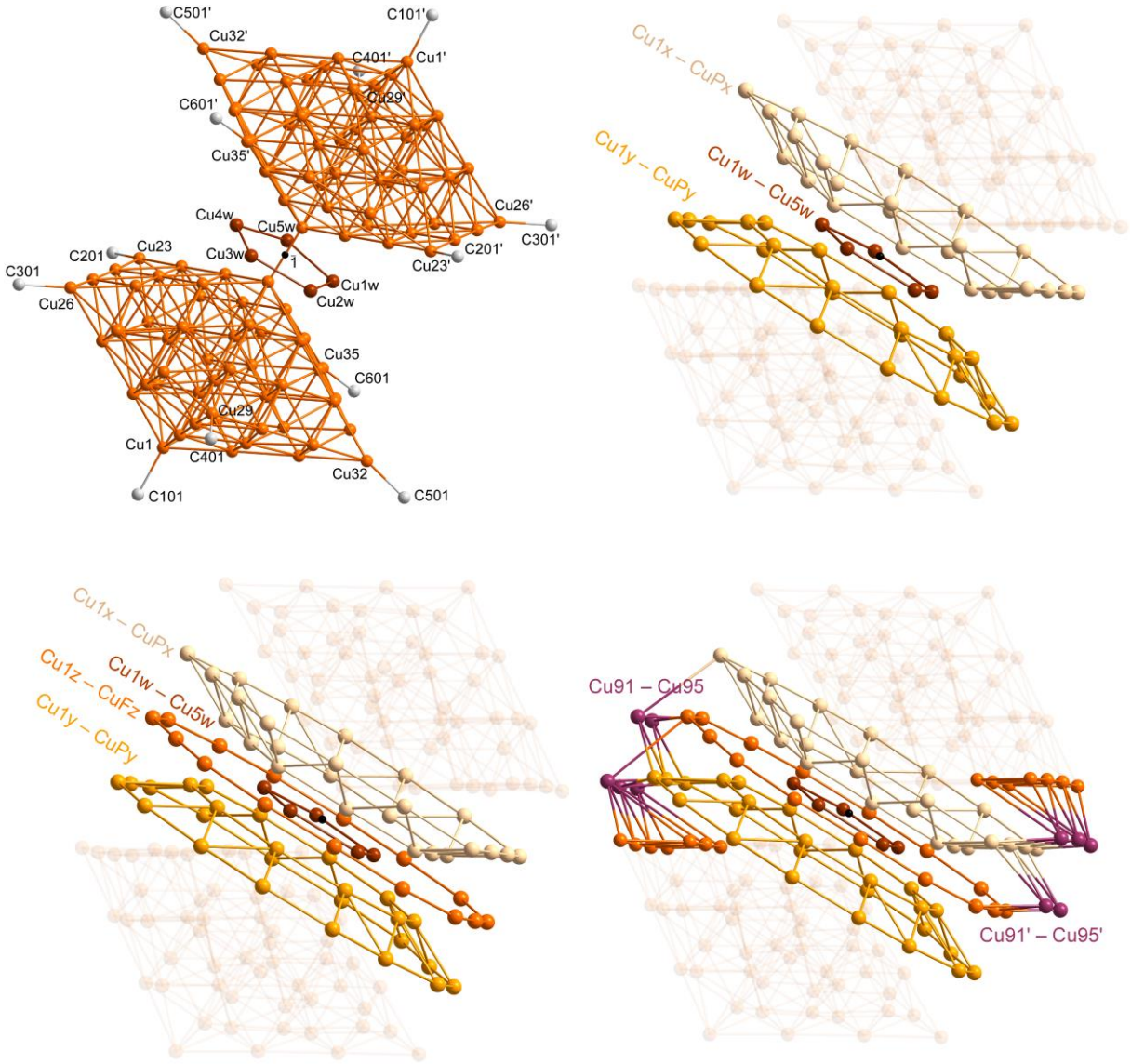

Figure S10: Selected details of the solid state structure of [(IDipp)$_{12}$Cu$_{179}$]. All atoms as spheres with arbitrary radii, prime indicates atoms generated by inversion, only the carbene carbon atoms of the NHC ligands are depicted.

Formally the structure of [(IDipp)$_{12}$Cu$_{179}$] may be constructed from different parts rationalising the discussed structure: The copper atoms Cu1–Cu54 forming a centrosymmetric dumbbell-like motif around the centre of inversion that exhibits approximate, non-crystallographic, five-fold symmetry along Cu1···Cu1'. To this centrosymmetric part all NHC ligands are coordinated via the carbene carbon atoms C101-601' (Figure S10, upper left). The centrosymmetry of the structure is broken by the five copper atoms Cu1w–Cu5w forming a (non-centrosymmetric) pentagon with the crystallographic inversion centre in its plane. This pentagon is the middle layer of the C_{19} motif discussed in the main text (Figure 5; Figure S10, upper left). The next

two motifs are two bowl-shaped, but distinct sets of 25 copper atoms, Cu1x–CuPx and Cu1y–CuPy, each (Figure S10, upper right). Of course, these two motifs are not readily identified from the corresponding electron density maxima. However, assuming that the entire cluster exhibits (approximate) five-fold symmetry and that Cu···Cu distances below 2.0 Å are implausible; these two distinct motifs are the only satisfying arrangement of these copper atoms. The last motif consist of a virtually planar ring of the 15 copper atoms Cu1z–CuFz with the centre on inversion within the plane (Figure S10, bottom left). Again, this motif is concluded under the given presumptions.

Finally, it is noted, that the four non-centrosymmetric motifs exhibit individual site occupancies of ½, in contrast to the site occupancy of the centrosymmetric part Cu1–Cu54 of unity.

Combining the five individual motifs, rejecting those combinations that led to Cu···Cu distances of below 2.0 Å as implausible led to only three plausible cluster structures. i) The combination discussed here, consisting of each motif once and the two combinations where either ii) Cu1x–CuPx *and* its symmetry related, inverted, counterpart *or* iii) Cu1y–CuPy *and* its symmetry related, inverted, counterpart are present. The latter two would imply that the crystal consists of two structurally distinct isomeric Cu_{178} motifs in a 1:1 ratio. Whereas, the former appears the more plausible explanation, the latter cannot be excluded from the crystallographic data.

Last, ten electron density maxima – pairwise symmetry equivalent – remained on the surface of the cluster. Assuming that these maxima represent partly occupied, disordered copper atoms (Cu91–Cu95) they refined freely to site occupancies of 0.189, 0.093, 0.038, 0.047, 0.144 (sum: 0.51) concluding a composition of $[(IDipp)_{12}Cu_{179}]$ (Figure S10, bottom right).

Nonetheless, it is again emphasised that the presence of hydrogen atoms, as additional ligand atoms cannot be ruled out from the diffraction data.

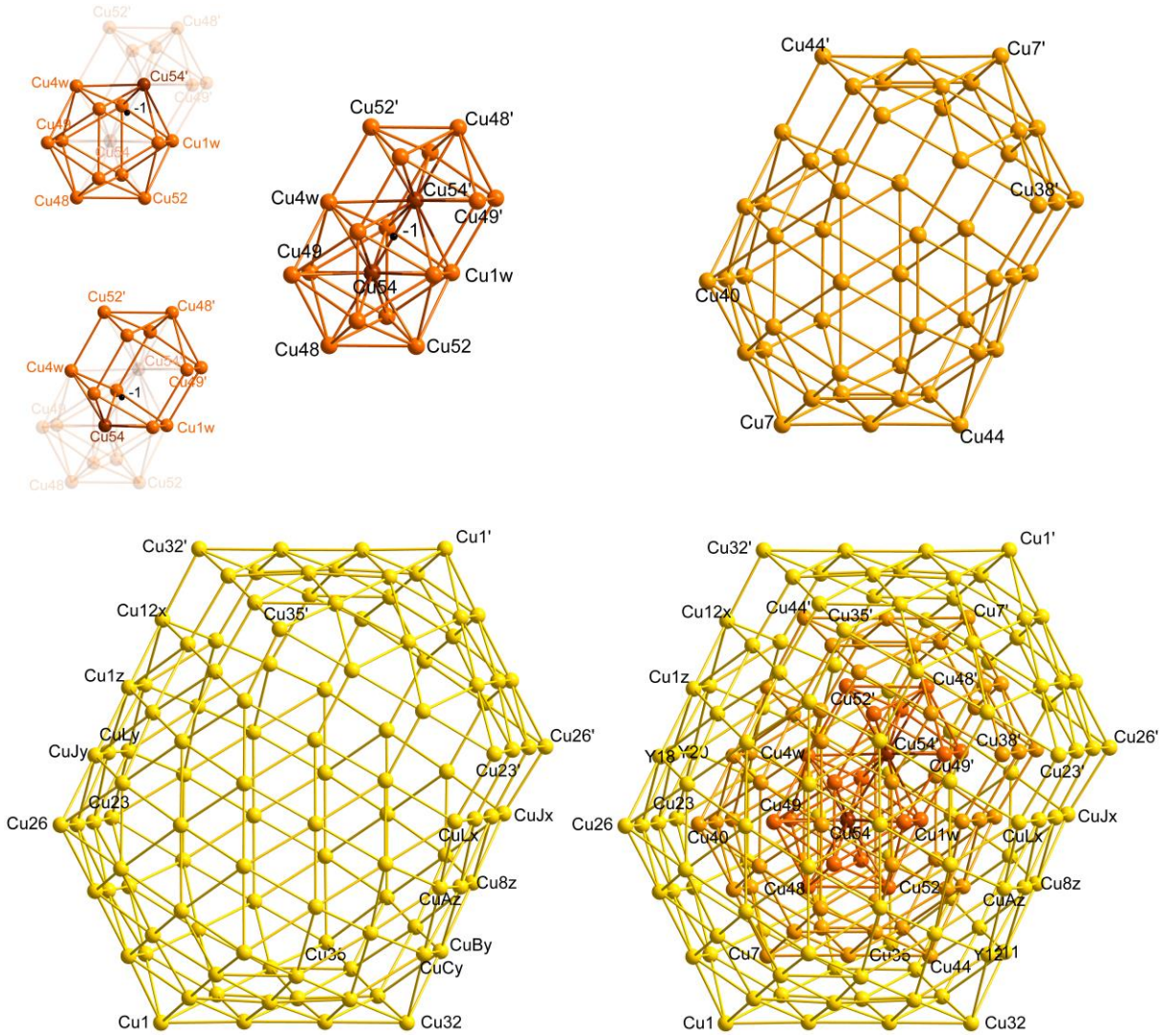

Figure S11: Selected details of the solid state structure of the Cu_{178} core within $[(IDipp)_{12}Cu_{179}]$. All atoms as spheres with arbitrary radii, prime indicates atoms generated by inversion. *Top left:* 1st shell and inner copper atoms (*insets:* highlighting the icosahedron and the capped pentagonal prism); *Top right:* 2nd shell; *bottom left:* 3nd shell; *bottom right:* inner Cu atoms, 1st, 2nd and 3rd shell superimposed.

An alternative view on the cluster core of $[(IDipp)_{12}Cu_{179}]$ is that it contains the same Cu_{55} motif as found in $[(IDipp)_6Cu_{55}]$. Around the centred icosahedron (on Cu54) a shell of 42 copper atoms is located (Figure S12). Hence, $[(IDipp)_{12}Cu_{179}]$ may be described as an extension of the Cu_{55} copper cluster found in $[(IDipp)_6Cu_{55}]$.

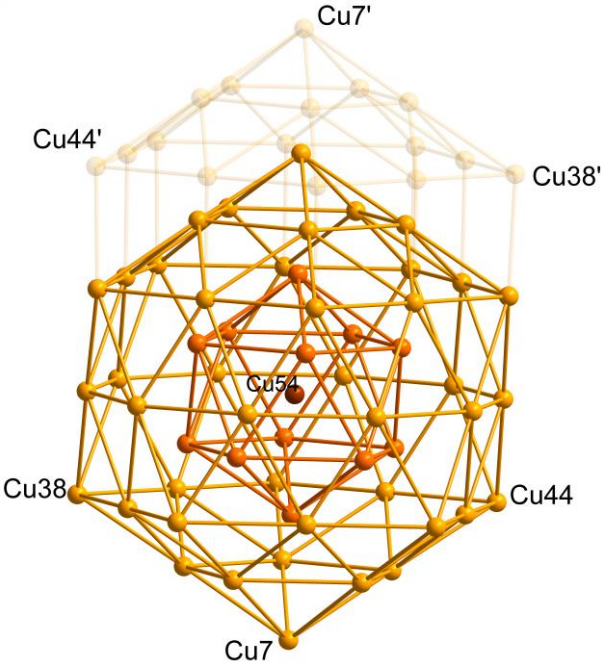

Figure S12: Selected view of the inner part of the Cu_{178} core (3rd shell removed) within $[(IDipp)_{12}Cu_{179}]$ emphasising the Cu_{55} motif analogue to $[(IDipp)_6Cu_{55}]$. All atoms as spheres with arbitrary radii, prime indicates atoms generated by inversion.

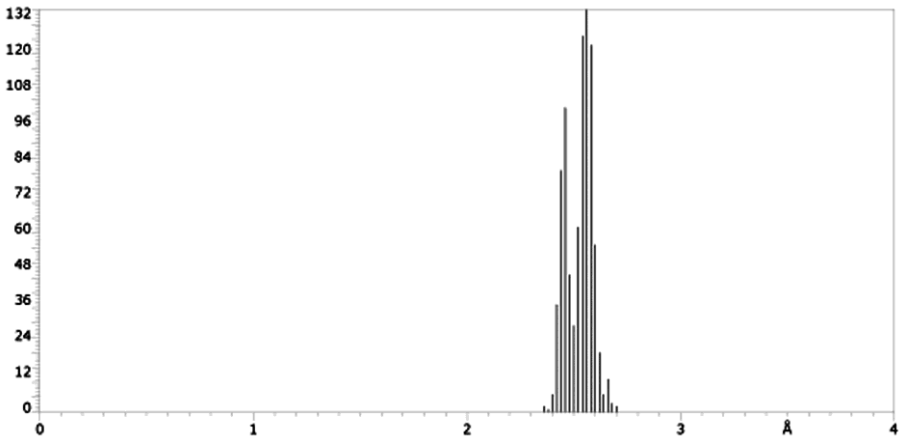

Figure S13: Histogram of the length of the direct Cu···Cu distances with the $[(IDipp)_{12}Cu_{179}]$ cluster, distances to and between the partly occupied copper atoms are not considered.

3a. Additional Full NMR Spectra of [(IDipp)Cu–Bneop] (**2**)

^{1}H NMR (500.3 MHz, THF-d_8, –40 °C)

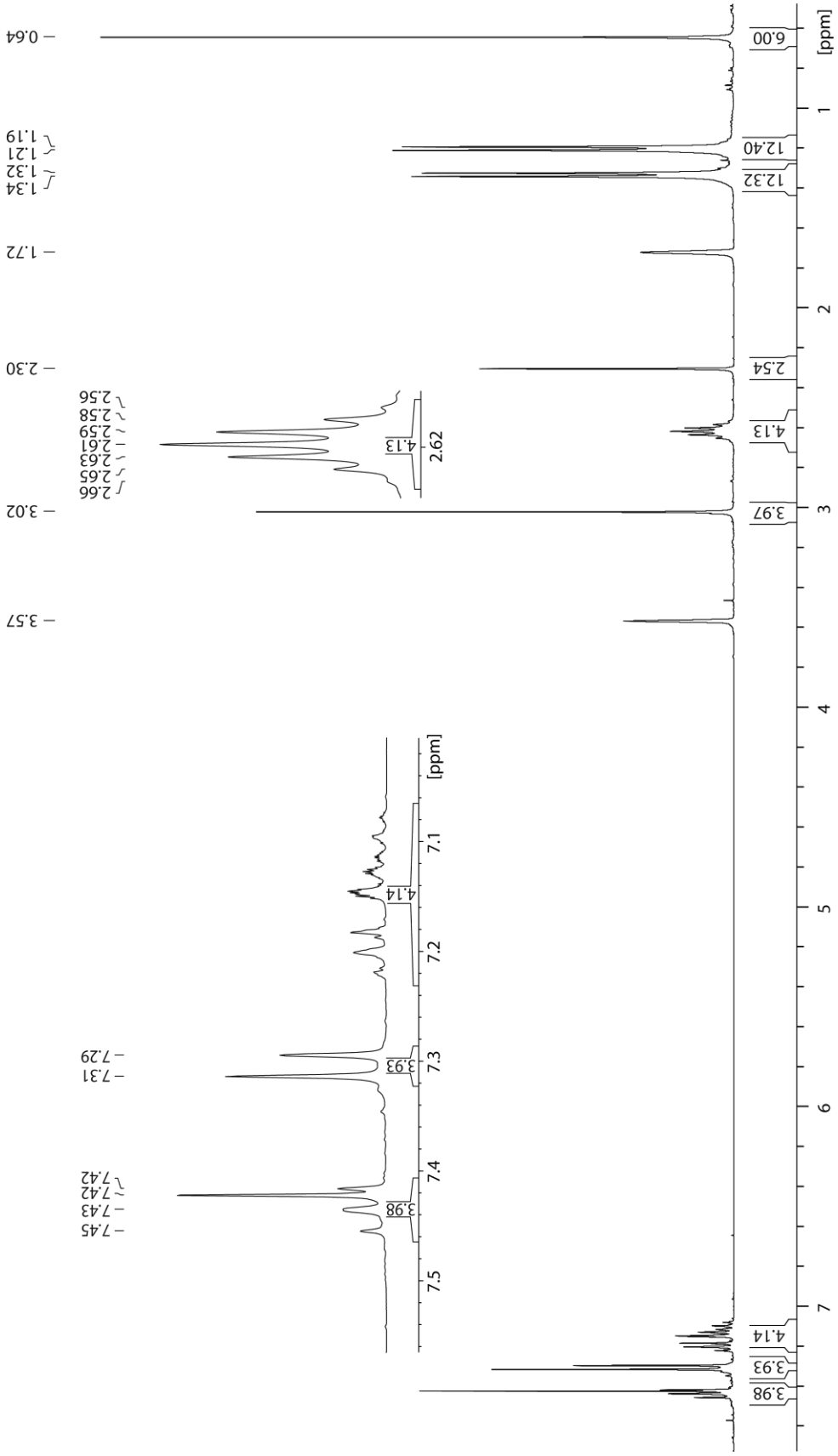

$^{13}C\{^{1}H\}$ NMR (125.8 MHz, THF-d_8, –40 °C), Inset: $^{13}C\{^{1}H\}$ DEPT NMR

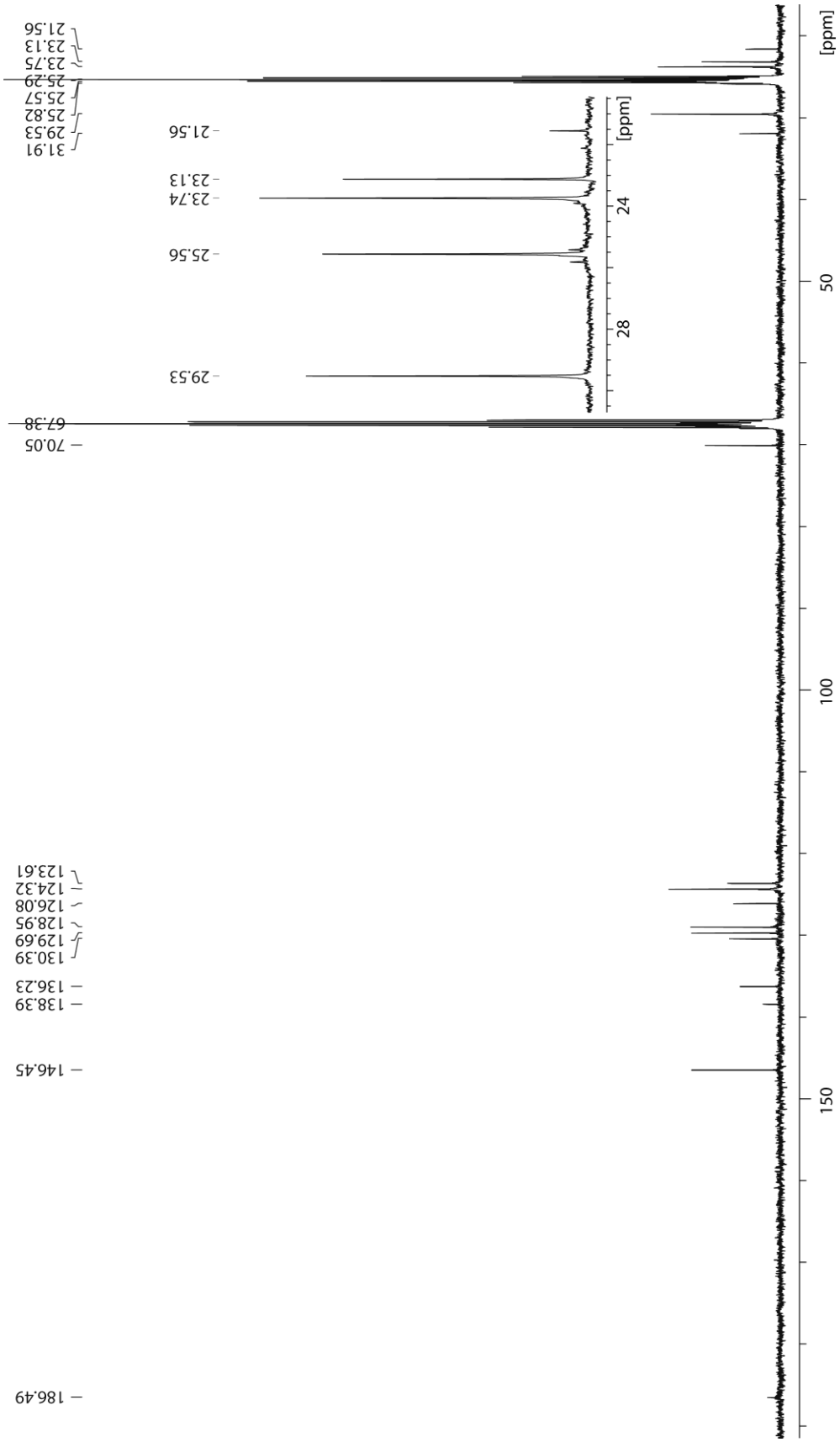

^{1}H NMR (600.1 MHz, C_6D_6, rt)

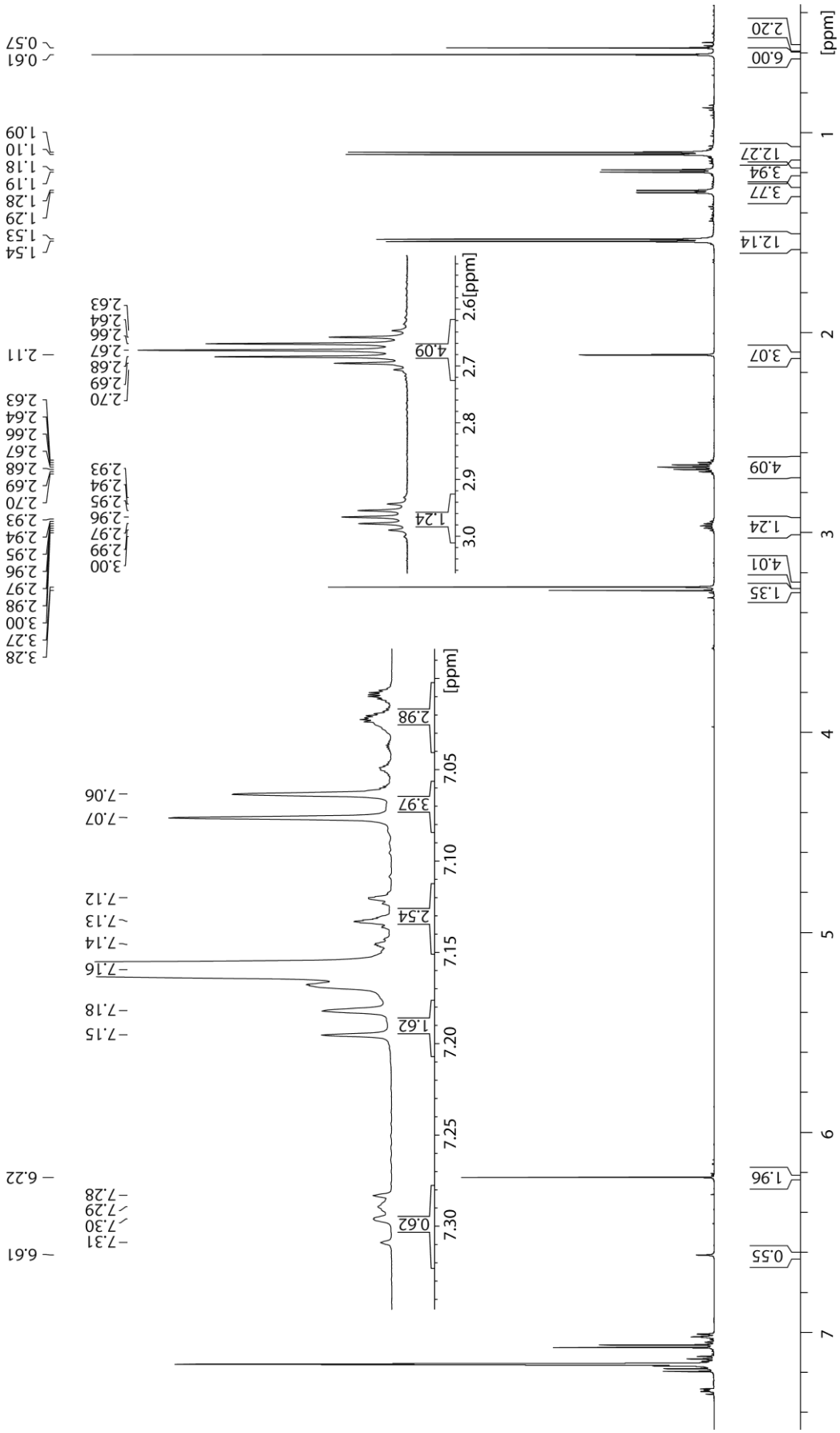

$^{13}C\{^{1}H\}$ NMR (150.9 MHz, C_6D_6, rt), left inset: $^{13}C\{^{1}H\}$ DEPT NMR

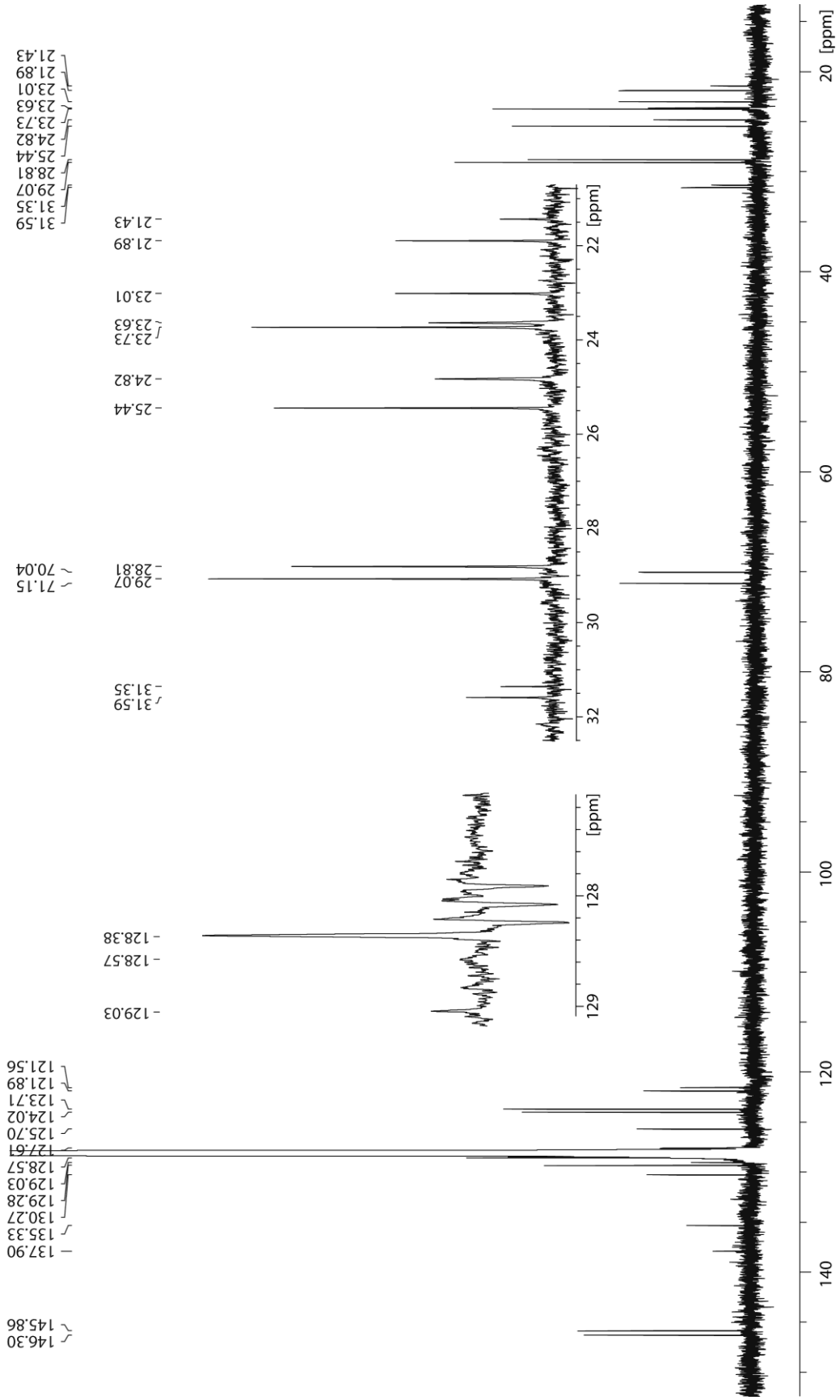

$^{11}B\{^{1}H\}$ NMR (96.3 MHz, C_6D_6, rt)

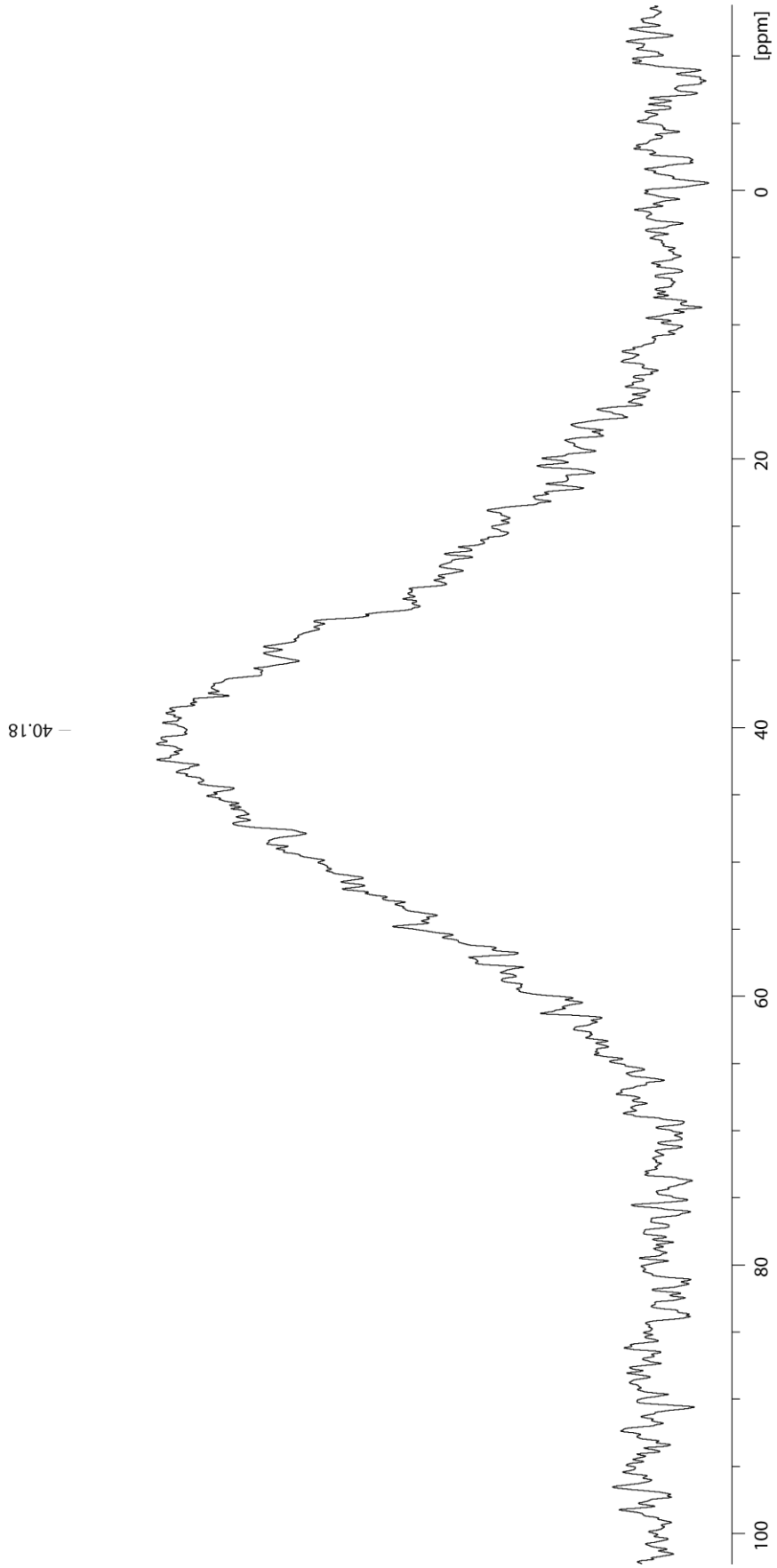

Decomposition Study **2** (^{1}H NMR, rt) and Spectra of Authentic Samples

3b. Additional Full NMR Spectra of [(IDipp*)Cu–Bneop] (**3**)

^{1}H NMR (300.1 MHz, C_6D_6, rt)

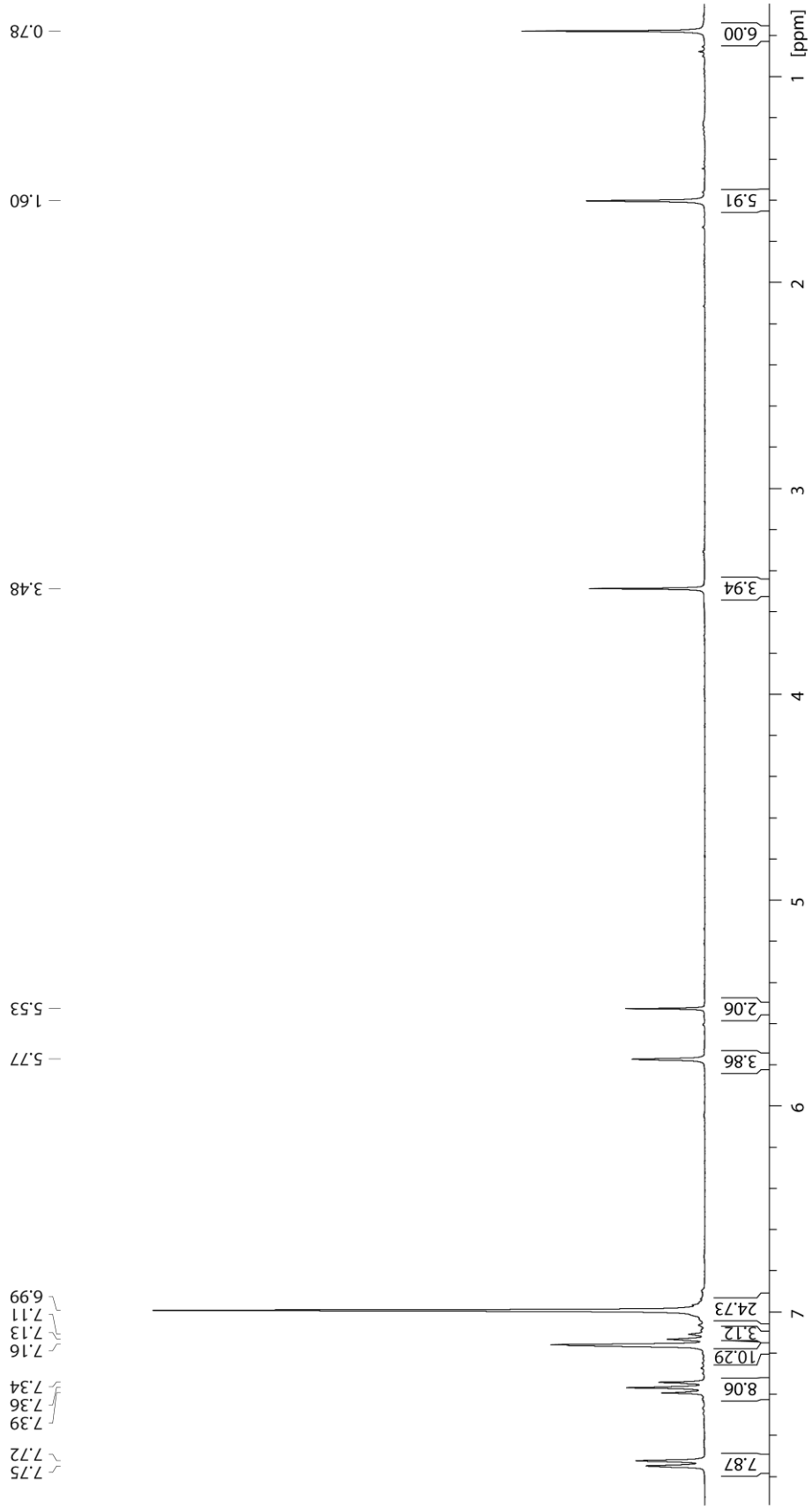

$^{13}C\{^{1}H\}$ NMR (100.7 MHz, C_6D_6, rt)

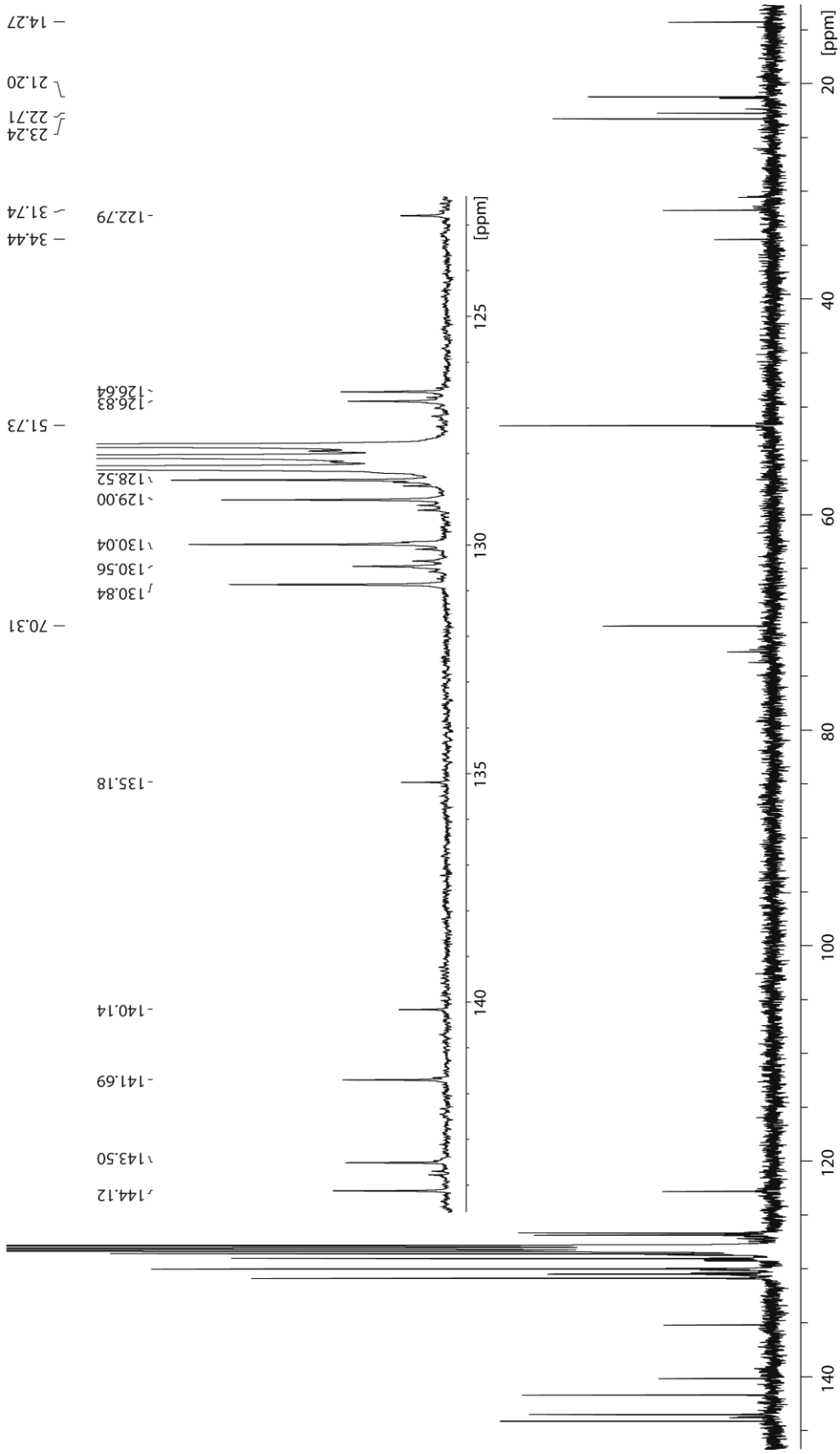

The signals at 14.3, 22.7 and 34.4 are assigned to an impurity of *n*-pentane. The carbene carbon atoms was only detected in a ^{1}H-^{13}C HMBC spectrum.

References:

[S1] IDipp: A. J. Arduengo III, R. Krafczyk, R. Schmutzler, H. A. Craig, J. R. Goerlich, W. J. Marshall and M. Unverzagt, *Tetrahedron*, 1999, **55**, 14523. B_2neop_2 (**1**): M. Eck, S. Würtemberger-Pietsch, A. Eichhorn, J. H. J. Berthel, R. Bertermann, U. S. D. Paul, H. Schneider, A. Friedrich, C. Kleeberg, U. Radius and T. B. Marder, *Dalton Trans.*, 2017, **46**, 3661. Cu: R. W. G. Wyckoff, *Crystal Structures*, 1963, **1**, 7.

[S2] A. L. Spek, *Acta Cryst.*, 2015, **C71**, 9.

[S3] P. van der Sluis and A. L. Spek, *Acta Cryst.*, 1990, **A46**, 194.

[S4] O. V. Dolomanov, L. J. Bourhis, R. J. Gildea, J. A. K. Howard and H. Puschmann, *J. Appl. Cryst.*, 2009, **42**, 339.